TECHNICAL ADVANCE

An aniline blue staining procedure for confocal microscopy and 3D imaging of normal and perturbed cellular phenotypes in mature *Arabidopsis* embryos

Sue Bougourd[1],*, Jo Marrison[1] and Jim Haseloff[2]

[1] *Department of Biology, University of York, PO Box 373, York YO10 5YW, UK, and*
[2] *Department of Plant Sciences, University of Cambridge, Downing Street, Cambridge CB2 3EA, UK*

Summary

A new method is described for fluorescent imaging of mature *Arabidopsis* embryos that enables their cellular architecture to be visualized without the need for histological sectioning. Mature embryos are stained with aniline blue and cleared with chloral hydrate to allow high-resolution confocal imaging of individual cells within the embryo prior to germination. The technique allows the collection of longitudinal optical sections throughout the cotyledon, hypocotyl and root of wild-type *Arabidopsis* C24 embryos. Every cell within the mature embryo can be visualized with sufficient clarity and resolution to allow three-dimensional analysis of cellular architecture. Optical sectioning of mutant *gnom, short-root and scarecrow* embryos, and through root meristems disrupted as a consequence of targeted misexpression of diphtheria toxin, demonstrate the potential of this technique for visualizing the cellular organization of mutant and perturbed embryonic phenotypes.

Keywords: *Arabidopsis thaliana*, embryo, confocal microscopy, 3D visualization, aniline blue, cellular architecture.

Introduction

The apical–basal body plan of the mature plant is established during embryogenesis; two meristems, root and shoot, are formed which subsequently determine the post-embryonic architecture of the plant. In order to understand plant morphogenesis, visualization of the cellular organization of developing plant organs is essential. For root development in *Arabidopsis thaliana*, much has been achieved by conventional histological techniques (Dolan *et al.*, 1993), which have provided an invaluable basis for subsequent interpretation of root morphogenesis. Alternatively, high-resolution optical sectioning by means of confocal laser-scanning microscopy can be used, circumventing the need for labour-intensive histological sectioning and allowing precise visualization of fluorescent signals within a narrow plane of focus by discarding light from out-of-focus regions. One difficulty, however, is that intact plant tissue consists of deep, alternating layers of refractile cell walls and aqueous cytosol, and contains various autofluorescent and light-scattering components (Haseloff, 1999). Mature embryos, which constitute an important and well defined stage in the transition between embryogenesis and post-embryonic growth, have been particularly difficult subjects for confocal microscopy. Even stains such as propidium iodide, which is used effectively for confocal imaging of *Arabidopsis* seedling roots (van den Berg *et al.*, 1995), cannot penetrate the dense tissues of the embryo. We describe here a new method for fluorescent imaging of mature *Arabidopsis* embryos that enables their detailed cellular architecture to be visualized simply and with a high degree of clarity. Mature embryos are stained with aniline blue and cleared with chloral hydrate to allow high-resolution confocal imaging of individual cells within the embryo prior to germination. We demonstrate that the images are of sufficient clarity and resolution to allow
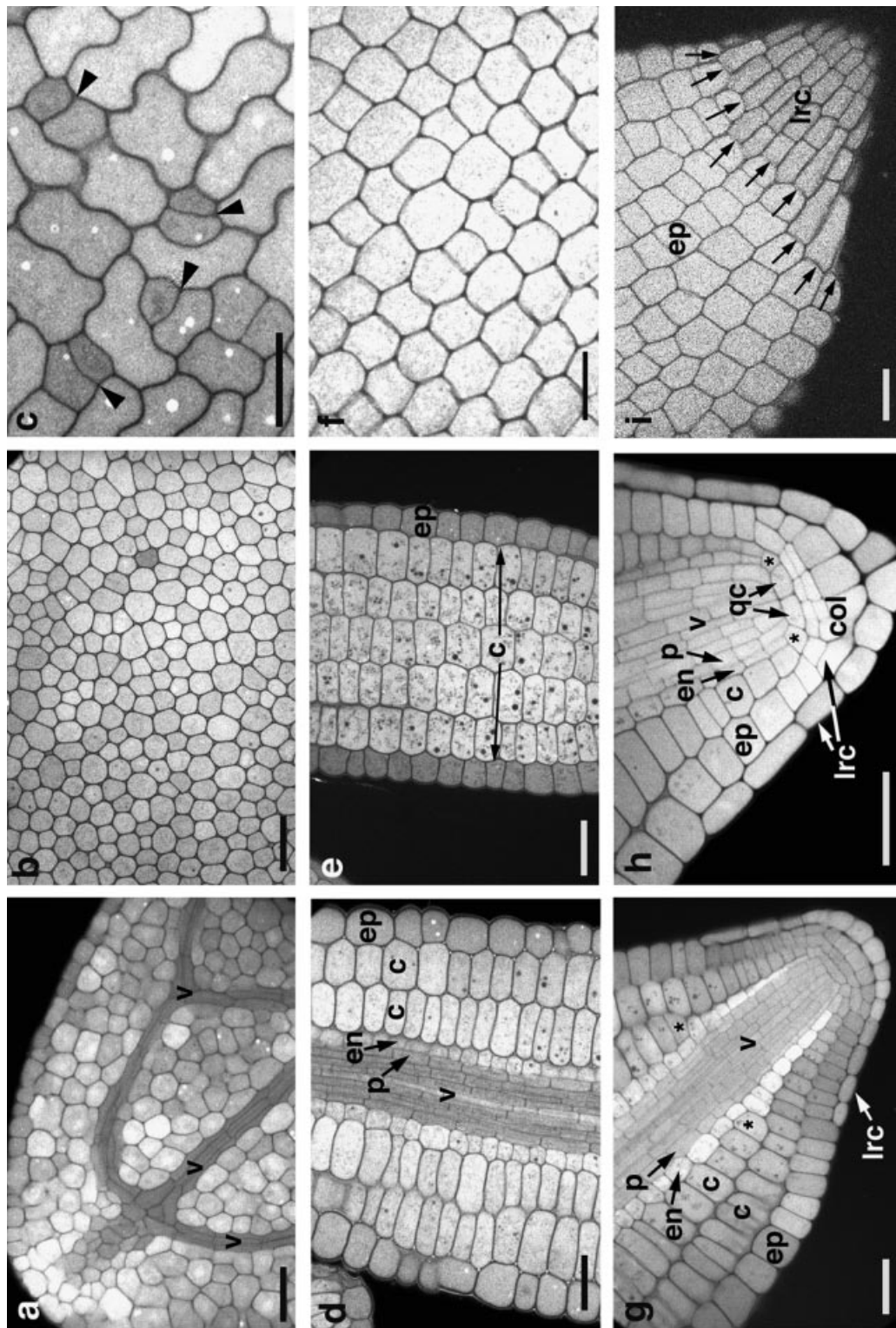
Figure 1. Confocal sections through aniline blue-stained mature embryos of wild-type *Arabidopsis thaliana* (C24): (a–c) cotyledon; (d–f) hypocotyl; (g–i) root.
(a) Median longitudinal section (MLS) through cotyledon, showing patterning and organization of vasculature. (b) Longitudinal section (LS) through epidermal layer of cotyledon. Arrowheads indicate asymmetric cell divisions, presumably representing divisions that will give rise to stomata. (d) MLS through hypocotyl, showing individual cell files. (e) LS through cortex of hypocotyl. Arrows delimit extent of cortical cells. (f) LS through epidermal layer of hypocotyl. (g,h) MLS through root, showing highly regular patterning. Asterisks mark (g) first cell of new cortical layer at the root/hypocotyl boundary; (h) endodermal/cortical initial cells. (i) LS through surface layers of root tip. Arrows show boundary of epidermis with lateral root cap. c, cortex; col, columella; en, endodermis; ep, epidermis; lrc, lateral root cap; p, pericycle; qc, quiescent centre; v, vascular bundle. Scale bar = 20 μm.
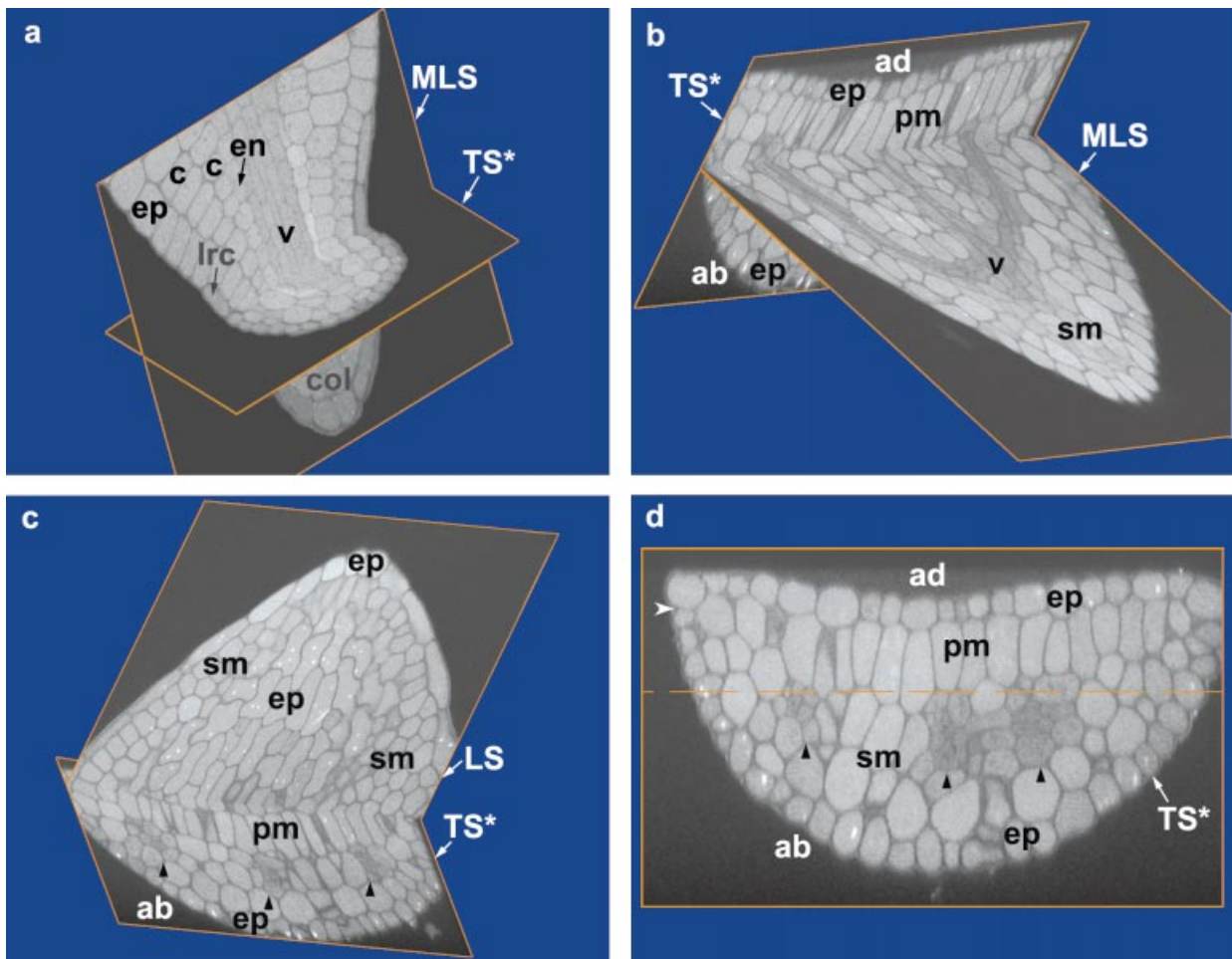
Figure 2. Three-dimensional reconstructions of transverse sections through embryonic root and cotyledon of wild-type *Arabidopsis thaliana* (C24): (a) embryonic root; (b–d) cotyledon.
(a) Median longitudinal section (MLS) through root and transverse section reconstructed from a Z-series of images (TS*), showing concentric layers of cells. (b) MLS through cotyledon and reconstructed TS*, showing morphology of different cell types. (c) Longitudinal section (LS) through upper cell layers of cotyledon taken at the level of the large arrowhead in Figure 2(d) and a reconstructed TS*. (d) Complete reconstructed TS* of cotyledon in which longitudinal section (at the position of the broken line) has been removed. ab, abaxial epidermis; ad, adaxial epidermis; c, cortex; col, columella; en, endodermis; ep, epidermis; lrc, lateral root cap; pm, palisade mesophyll; sm, spongy mesophyll; v, vascular bundle. Arrowheads in (c) and (d) show positions of vascular strands.

reconstruction of the three-dimensional cellular architecture of embryos. In addition, we show that the technique can be applied to the analysis of aberrant cell arrangements in *Arabidopsis* mutant embryos, and can be used to visualize the consequences of perturbed development such as that caused by targeted misexpression of genes in particular cells of developing meristems using GAL4/enhancer trap approaches.

Results

Wild-type C24 Arabidopsis

Mature embryos, removed from their seed coats, were stained with aniline blue and cleared in chloral hydrate as

described under Experimental procedures, and observed using laser-scanning confocal microscopy.

Optical sections through the cotyledon, hypocotyl and root reveal the high level of detail with which the organization of different cell layers can be visualized (Figure 1). A median longitudinal section through the cotyledon (Figure 1a) shows clearly the patterning and organization of the vasculature, with a central vein and interconnecting side branches. Longitudinal sections through the mesophyll and epidermal cell layers (Figure 1b,c) reveal the precise shapes and distribution of cells, and show evidence of asymmetrical cell divisions amongst the jigsaw-shaped cells of the epidermis, presumably representing the divisions that give rise to stomata (Figure 1c).

A median longitudinal section through the hypocotyl (Figure 1d) allows the regular organization of cells to be
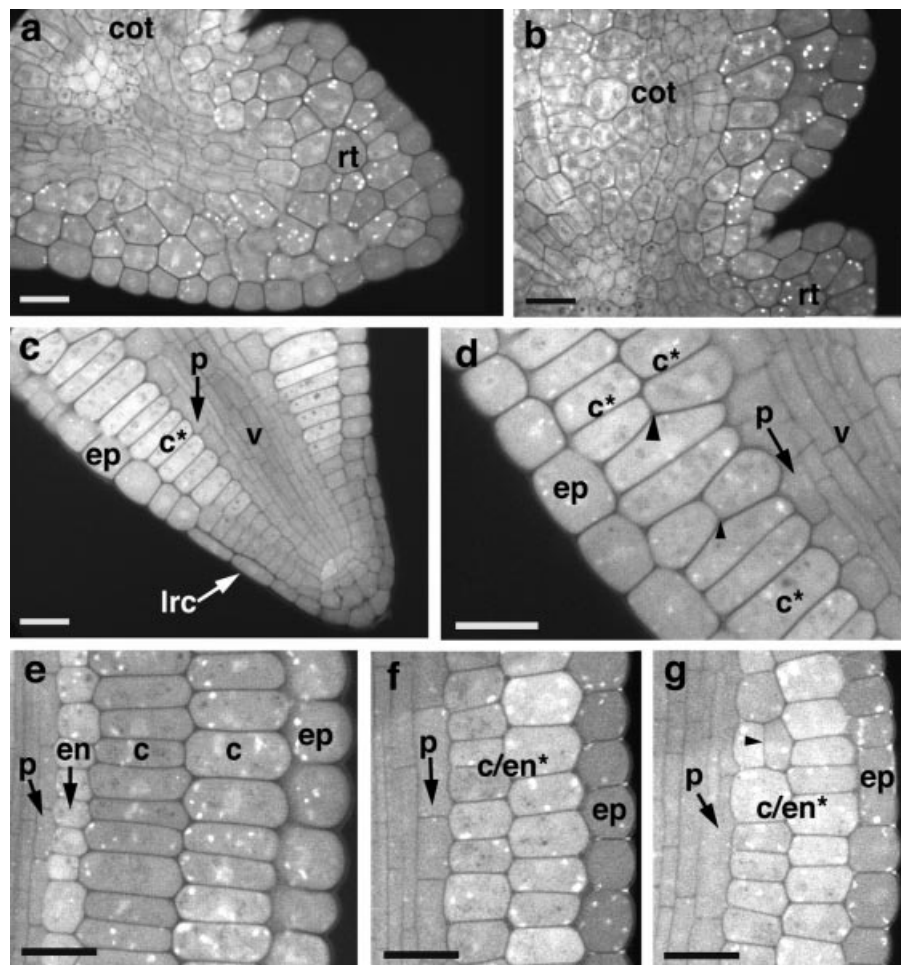
Figure 3. Confocal sections through aniline blue-stained mutant embryos.
(a,b) Longitudinal section (LS) through *gnom*, showing some regional differentiation into root (a) and shoot (b). (c) Median longitudinal section (MLS) through *short-root,* showing a single layer of cortical cells between epidermis and pericycle in root and hypocotyl. (d) MLS through *short-root* in the upper region of the hypocotyl. Small arrowhead, position of an isolated periclinal division in the cortex. Division of single cortical cell file into two distinct files appears to occur beyond this point (large arrowhead). (e) MLS through hypocotyl of a wild-type (C24) embryo, showing normal ground tissue cell files, i.e. two cortical and an endodermal layer. (f,g) MLS through hypocotyl of *scarecrow,* showing two instead of three cell files between epidermis and pericycle. Arrowhead in (g), position of an isolated supernumerary periclinal cell division in one of the mutant layers. cot, cotyledon; rt, root; c, cortex; c*, mutant cell layer with cortical attributes; c/en*, mutant cell layer with cortical and endodermal attributes; en, endodermis, ep, epidermis; lrc, lateral root cap; p, pericycle; v, vascular bundle. Scale bar = 20 μm.

visualized. The vascular, pericycle, endodermal, cortical and epidermal files of cells are clearly identifiable (Figure 1d). Non-median longitudinal sections highlight the regularity of the cortical (Figure 1e) and epidermal (Figure 1f) cells. It is easy to see the point at which the second cortical layer is formed, a short distance from the tip, which occurs consistently just beyond the end of the lateral root cap (asterisks in Figure 1g). This region demarcates the end of the embryonic root and the beginning of the hypocotyl.

In addition to cell types found in the hypocotyl, a median longitudinal section through the root reveals cells of the quiescent centre, four rows of columella cells, and two outer layers of lateral root cap cells (Figure 1h). It is also possible to identify the origin of the cortical and endodermal cell files close to the root tip, resulting from the formative cell division of the daughter cells of the endodermal/cortical initial cells (asterisks in Figure 1h). In longitudinal sections through the surface layers of the root, note particularly how the epidermal cells give way to lateral root cap cells at the root tip (Figure 1i). The two most distal rows of lateral root cap cells appear to form more-or-less concentric rings, whilst the more proximal rows appear to have less synchronous divisions.

Figure 2 illustrates how transverse sections can be reconstructed, using appropriate software, from a Z-series of images taken through the longitudinal plane of mature embryonic organs. For the root, a median longitudinal section is displayed, with a coronal transverse section reconstructed at a level approximately half-way between the tip and the end of the lateral root cap (Figure 2a). The reconstructed transverse section reveals concentric layers of cells, from the central vascular cells, through the pericycle, endodermis, cortex and epidermis, to the lateral root-cap cells.

For the cotyledon, a median longitudinal slice (Figure 2b) and a longitudinal slice through the upper cell layers (Figure 2c) are displayed, together with transverse sections reconstructed from a Z-series of images through the longitudinal axis approximately half-way from the tip of the organ. Figure 2(d) shows an entire transverse section reconstructed from longitudinal sections. It is possible in all cases to distinguish individual cells and cell layers,
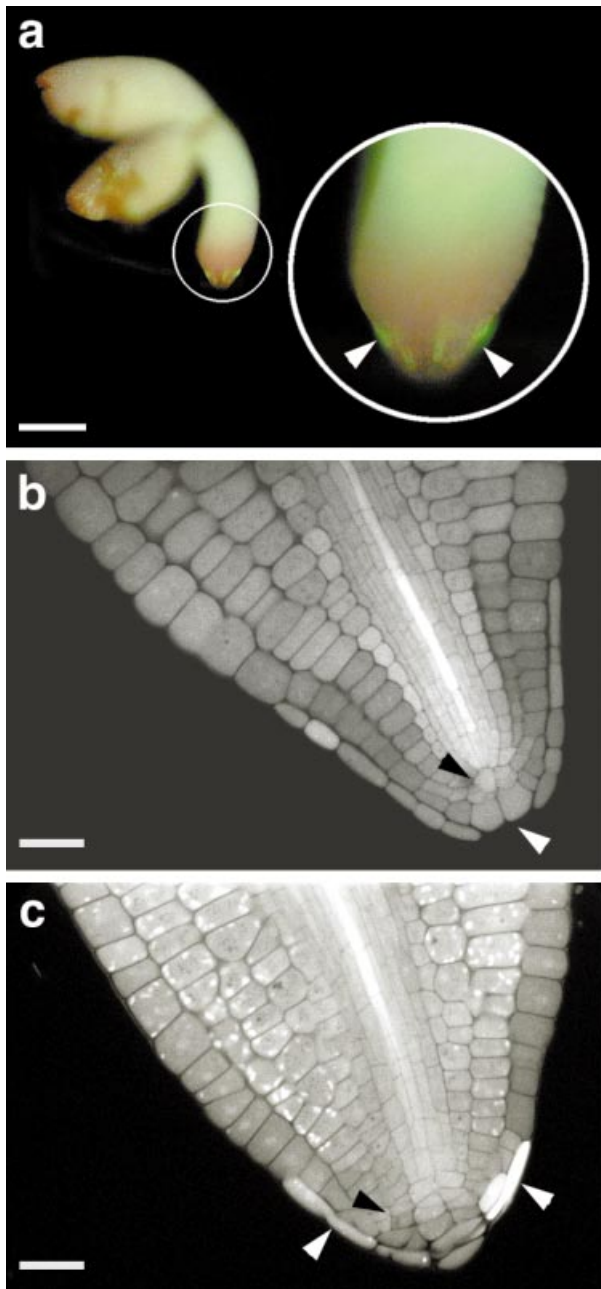
(Figure 2b–d). Three vascular bundles are evident within the mesophyll at the level of the reconstructed transverse sections (Figure 2b–d).

Mutant embryos

To further test the technique, we examined mutants of *Arabidopsis*: *gnom* (Mayer *et al.*, 1993); *short-root* (Benfey *et al.*, 1993); and *scarecrow* (Di Laurenzio *et al.*, 1996; Scheres *et al.*, 1995), that possess altered cell arrangements in the mature embryo. Mutant embryos were stained, cleared and observed in the same way as for the normal C24 embryos. The cellular architecture of the mutant pheno-types can be visualized clearly, especially in the case of mutations that perturb the root system with its simple, well defined arrangement of cells, as shown in Figure 3.

In the case of the *gnom* mutant embryo shown in Figure 3(a,b), a severe reduction of apical and basal end regions is evident. Some regional differentiation into 'root' (Figure 3a) and 'cotyledon' (Figure 3b) has occurred, but the mutant lacks normal root-cell files and hypocotyl, and has ill-formed vascular strands. In *short-root* mutant embryos, a single layer of cells, rather than the normal cortex and endodermis, is evident between the epidermis and peri-cycle in the root (Figure 3c), and two layers rather than the usual double cortical layer and endodermis can be seen further up in the hypocotyl (Figure 3d). Abnormal cell divisions are evident in the affected layer, with isolated periclinal divisions occurring that do not result in two distinct continuous cell files (Figure 3d). A close-up of the normal hypocotyl cell files in the wild type (Figure 3e) can be contrasted with the cell files of *scarecrow* mutant embryos (Figure 3f,g). In *scarecrow*, the absence of a cell layer can be readily detected, with two layers rather than three between the epidermis and pericycle in the region of the hypocotyl illustrated in Figure 3(f,g). Note that the columnar-shaped layer of cells adjacent to the vascular cells, which we assume from previously published descrip-tions of the *scarecrow* phenotype to be pericycle cells (Di Laurenzio *et al.*, 1996; Scheres *et al.*, 1995), are consider-ably wider than normal (Figure 3f,g). Supernumerary periclinal divisions in the affected root-cell layers are also clearly evident in *scarecrow* (Figure 3g).

GAL4 targeted cell ablation

We also tested the technique on embryos that had been disrupted as a consequence of targeted misexpression of diphtheria toxin (see Experimental procedures). Again, the cellular organization of perturbed embryos could be readily visualized.

Figure 4 shows the consequences of genetic crossing between the GAL4 line J1103 and a line in which the diphtheria toxin A chain gene (*DT-A*) has been placed under

Figure 4. Transactivation of diphtheria toxin A chain (DT-A) in embryos of GAL4 line J1103.
(a) Epifluorescence image of a whole, mature J1103 embryo showing GAL4 expression marked by green fluorescent protein (GFP). Localization of GAL4 and GFP expression can be seen specifically in the root-cap region of the embryo (arrowheads, inset). (b,c) Median longitudinal sections through J1103 embryos in which DT-A has been transactivated, showing ablation (white arrowhead) of columella cells (b) and lateral root cap cells (c), and disruption of cell divisions in neighbouring columella cells (black arrowhead). Scale bars: (a) = 200 μm; (b,c) = 20 μm.

including the epidermal cells, and a layer of columnar-shaped palisade mesophyll cells adjacent to the adaxial epidermis and two or three layers of more rounded, spongy mesophyll cells adjacent to the abaxial epidermis

the control of GAL4 upstream activator sequences. J1103 expresses GAL4 during embryogenesis in the outer layers of the columella and in the lateral root cap (Figure 4a). It is clear that activation of *DT-A* in these cells leads to ablation of cells within corresponding regions of the root cap of the mature embryo (Figure 4b,c). Note how clearly the resulting absence of the lower columellar cells can be seen using this technique (Figure 4b), and how easily ablated cells in the lateral root cap can be identified (Figure 4c). It is also possible to visualize the disruption of cell-division planes in neighbouring cell layers, causing serious disruption of embryonic root cellular architecture (Figure 4b,c).

Discussion

We have developed a new staining procedure, involving staining with aniline blue and clearing with chloral hydrate, that allows detailed visualization of the cellular architecture of mature *Arabidopsis* embryos without the need for histological sectioning. Thin sectioning is laborious, and the problems of obtaining sections in the desired plane, and of obtaining a complete series of sections through the whole embryonic organ, have limited its use to experienced laboratories. Optical sectioning deep into plant tissues can also be difficult due to light scattering and spherical aberration caused by particulate subcellular matter and refractile cell walls, but we have overcome this by clearing the stained embryos with a high-refractive-index mountant containing chloral hydrate. The aniline blue technique described here allows optical rather than histological sectioning which has many advantages, not least of which are speed and simplicity.

Commercial aniline blue preparations are heterogeneous mixtures of various components, including a fluorochrome that has its excitation maximum in the UV range and a maximum emission at around 455 nm (Smith and McCully, 1978). Aniline blue has been used for many years as a stain for callose in plant cells (Currier, 1957), and has been particularly valuable in observations of pollen tubes within the style (Alexander, 1987; Kho and Baer, 1968; Martin, 1959) and microsporocytes (Alche and Rodriguez-Garcia, 1997). Nickle and Meinke (1998) used aniline blue to observe excessive callose accumulation in a cytokinesis-defective mutant of *Arabidopsis*, *cyt1*, and confirmed this using Sirofluor, a callose-specific UV-excited fluorochrome derived from aniline blue preparations (Ahlborn and Werner, 1992; Stone *et al.*, 1984).

In this work we show that aniline blue also provides a fluorochrome that is excited by longer-wavelength visible light, and will selectively stain the cell contents of mature embryos. The 514 nm line of an argon ion laser can be used to excite aniline blue-stained embryos for laser-scanning confocal microscopy with a red emission, and this has been shown to be reproducible using several batches of aniline blue from different sources. Although aqueous solutions of aniline blue fluoresce only relatively weakly at these longer wavelengths when excited at 514 nm (data not shown), it is possible that the fluorescent properties of aniline blue are altered after binding to the plant material, as observed by Smith and McCully (1978).

We have demonstrated in this paper the potential of the aniline blue staining technique as a tool for visualizing the two- and three-dimensional cellular arrangements of wild-type, mutant and perturbed embryonic phenotypes in *Arabidopsis*. In wild-type embryos, optical confocal sections through the longitudinal axis enable individual cells of all the different cell layers to be visualized in the embryonic root, hypocotyl and cotyledon. A series of optical Z-sections, taken every 0.2 µm along the longitudinal axis of the embryonic root and cotyledon, can be captured, and the large data sets (approximately 200 MB in size) processed by 3D reconstruction software packages such as AMIRA (Indeed-Visual Concepts GmbH, Berlin). We have demonstrated that the clarity and resolution of the optical sections allow full reconstruction of coronal transverse sections, again in sufficient detail to identify individual cells. Three-dimensional visualization software can process these large confocal data sets further, enabling individual cells to be segmented and rendered in three dimensions (Bougourd and Haseloff, unpublished data).

We have also demonstrated that this technique works well for aberrant phenotypes, and offers the opportunity of analysing the detailed cellular architecture of mutant phenotypes at the mature embryonic stage. The mutants included in this study to test the efficacy and potential value of the aniline blue staining procedure in analysing cellular architecture were *gnom*, *short-root* and *scarecrow*.

GNOM is a gene required for pattern formation along the apical–basal axis in the *Arabidopsis* embryo (Mayer *et al.*, 1993). Aniline blue staining and confocal sectioning enabled visualization of the internal embryonic architecture of this mutant, even in severely disrupted phenotypes. In the embryo shown in Figure 3, there was a very substantial reduction in the development of an apical–basal axis, although some regional differentiation into root and cotyledon had occurred. However, there was clearly no evidence of normal root-cell files or a hypocotyl, and the vascular strands were ill-formed. Based on the shape and regional differentiation of the seedling (Figure 3a,b), the embryo belongs to the so-called 'oblong' phenotypic class (Mayer *et al.*, 1993). Despite severe disruption of the embryo, it proved possible to visualize individual cells and cellular patterning simply and clearly, using the aniline blue approach.

Short-root and *scarecrow* are radial-pattern mutants in which only a single layer of cells is present between the epidermis and pericycle of the root, instead of the normal cortical and endodermal layers. In *short-root,* the single

remaining layer lacks endodermal differentiation markers (Benfey *et al.*, 1993; Scheres *et al.*, 1995), but has cell-specific cortical attributes (Helariutta *et al.*, 2000), whereas in *scarecrow*, cell-specific markers of both cortex and endodermis are present (Di Laurenzio *et al.*, 1996; Scheres *et al.*, 1995). Morphological characterization of the mutant phenotypes has previously involved transverse sectioning of plastic-embedded material (Di Laurenzio *et al.*, 1996; Scheres *et al.*, 1995), and Nomarski optical sections of mutant seedlings (Di Laurenzio *et al.*, 1996). Our technique has enabled clear visualization in the root of a single layer of cells between the epidermis and pericycle in both *short-root* (Figure 3c,d) and *scarecrow* (not illustrated). This was achieved without physical sectioning, and with considerably greater contrast and resolution than is possible in Nomarski optical sections of embryos. In the hypocotyl of *short-root* and *scarecrow*, the single aberrant layer appears to divide into two files of cells, still resulting in a missing layer of cells compared with wild-type (Figure 3d,f,g). In the affected cell layers of *short-root and scarecrow* embryos, the technique also revealed the presence of individual cells that had undergone aberrant periclinal division. These divisions tended to occur in isolated cells and did not result in two distinct continuous cell files. The presence of such periclinal divisions in affected files of cells was originally thought not to occur in *scarecrow*, but has recently been reported by Wysocka-Diller *et al.* (2000). We confirm the occurrence of such divisions in *scarecrow* (Figure 3g), and report here also the occurrence of a similar phenomenon in *short-root* mutant embryos (Figure 3d).

We also show that, using this procedure, we can visualize the consequences of deliberate perturbation of normal cellular architecture. Specifically, we have demonstrated that the effects on cellular architecture of targeted cell ablation can be visualized in the mature embryo, with respect to both the targeted cells and their neighbours (Figure 4b,c). The diphtheria toxin A chain (DT-A) can be transactivated in particular cells by crossing a GAL4-dependent *DT-A* transgenic line to selected GAL4-enhancer trap lines. In the example described here, ablation of cells in and around the area of the columella and root cap has been achieved, corresponding to the expression pattern of GAL4 and GFP in the enhancer trap line used (Figure 4a). These ablated cells can be visualized clearly and simply in the embryo by confocal optical sectioning of stained roots, as can the aberrant cell division planes in neighbouring columella cells, present presumably as a consequence of the ablation of adjacent columella and lateral root cap cells (Figure 4b,c).

In conclusion, we have developed a new staining technique for mature *Arabidopsis* embryos that combines the capacity of aniline blue to be excited using the 514 nm laser line of the confocal microscope and clearing with the high-refractive-index agent chloral hydrate, to allow high-resolution imaging of individual cells. Optical sectioning of aniline blue-stained embryos by confocal microscopy is quick and relatively straightforward, and the method allows imaging through the entire *Arabidopsis* embryo without requiring physical sectioning. Simple, routine visualization of longitudinal sections through embryonic organs can be readily applied to the investigation of wild-type, mutant and experimentally perturbed phenotypes. Computer visualization software can be used for the 3D reconstruction of entire embryonic organs, and is demonstrated here for wild-type embryonic roots and cotyledons. The same procedures can also readily be applied to mutant embryos, and are currently being used by us for reconstruction and analysis of meristems that have been genetically perturbed by GAL4-targeted misexpression.

Experimental procedures

Plant materials

Wild-type *Arabidopsis thaliana* seeds, ecotype C24 (Valvekens *et al.*, 1988), were from stocks maintained in J.H.'s laboratory. Mutant *gnom* seeds were obtained from the *Arabidopsis* Biological Resource Centre, and *short-root* (*shr-1*) and *scarecrow* (*scr-1*) seeds were kindly provided by Philip Benfey (New York University, NY, USA).

Seeds of the GAL4 line J1103 were from stocks available in J.H.'s laboratory (http://www.weed3D.com). J1103 is one of a library of *Arabidopsis*-enhancer trap lines, generated by Haseloff (1999) and colleagues, that express the transcription activator GAL4-VP16 in different patterns within the developing plant; the presence of a GAL4-responsive *mGFP5* gene (Haseloff *et al.*, 1997) acts as an immediately detectable vital marker. Any gene of interest can be placed under the control of GAL4 upstream activator sequences (UAS), and become specifically activated in particular cells or tissue types by genetic crossing to one of the GAL4 lines.

In the work described here, J1103 plants were crossed to a transgenic line in which the gene for diphtheria toxin A chain (*DT-A*) had been engineered to be dependent on the presence of GAL4 for its expression (J. Haseloff, unpublished results). Thus DT-A is transactivated within the *Arabidopsis* embryo in order to cause targeted cell ablation, specifically in cell layers expressing GAL4 and GFP.

Staining procedure

Seeds were imbibed overnight in water at 4°C. They were transferred to a lightly moistened Millipore Petri-Pad (PD10047S5) (Millipore UK Ltd, Watford, Herts, UK), and the seed coats were removed under a dissecting microscope using fine forceps (number 5) and microneedles (250 μm). The naked embryos were transferred to a cell strainer (Falcon 2350, 70 μm nylon mesh, Becton Dickinson Labware Europe, Le Pont de Claix, France) sitting in a well of a six-well plate (Falcon 3046) containing 15% (v/v) ethanol. The embryos were then dehydrated through an ethanol series (15, 50, 70 and 96%, and two changes of 100% (v/v) ethanol), 15 min in each. The ethanol was removed by aspiration from the well around the strainer, and fresh 100% ethanol gently added directly to the strainer, minimizing damage to the embryos.

The embryos were left in 100% (v/v) ethanol at 4°C, usually overnight (or for at least 3 h). They were rehydrated in a similar way through 96, 70, 50 and 15% (v/v) ethanol, 15 min in each, and finally through two changes of fresh deionized water, 15 min in each. 0.5% (w/v) aniline blue stock solution was made by dissolving aniline blue, water soluble, colour index (C.I.) 42755 (BDH 'Gurr' 34003 4C, Merck Ltd, Poole, Dorset, UK, or Sigma A-9016, Sigma-Aldrich Co. Ltd, Poole, Dorset, UK or TAAB SD015/25) in 0.2 M phosphate buffer pH 6.5 or deionized water, and filtering through Whatman no. 1 paper. The embryos were stained in a 1 in 20 dilution of the stock solution for 30 min, rinsed well (but gently) with water to remove unbound aniline blue, then soaked in two changes of water, 15 min in each. The embryos were dehydrated and then rehydrated again through the ethanol series as described above. Embryos were transferred to clean microscope slides (Blue Star Microslides (washed), 76 × 26 mm, 1.0/1.2 mm thick, Chance and Propper, Warley, UK), and mounted in Hoyer's solution [30 g gum arabic (Sigma G-9752), 200 g chloral hydrate (Sigma C-8383), 20 g glycerol, 50 ml water] once any excess water had evaporated. A cover slip (22 × 50 mm, 0 thickness, Chance and Propper, Warley, UK) was gently lowered on to the mountant, taking care to minimize the creation of air bubbles around the embryos. In order to avoid any risk of crushing the embryos during microscopy, slides were left undisturbed for several days until the Hoyer's solution had hardened.

Microscopy

Optical sections were obtained using Nikon Optiphot-2 upright microscopes, equipped with either a Bio-Rad MRC-600 or a Bio-Rad MRC-1000 scanhead (Bio-Rad Laboratories Europe Ltd, Hemel Hempstead, Herts, UK). The 514 nm excitation line of a 25 mW argon ion laser was used, and laser power was reduced to 3% intensity by means of neutral density filters. The images shown were taken through Nikon planapo 60× oil immersion objectives (NA 1.4, WD 0.17 mm). Signals were collected either through a GHS (DR540LP) filter block with a 550 nm long pass emission filter, or through an A1 (DR527LP)/A2 (DR565LP) filter block set with a 585 nm long pass emission filter (all filters supplied by Bio-Rad). Kalman averaging was carried out over 20 frames for single images and over five frames for Z-series images. Z-series images were collected at 0.2 μm intervals through the specimens. Images were processed using the software CONFOCAL ASSISTANT (BioRad) and ADOBE PHOTOSHOP (version 5.5), and AMIRA (Indeed-Visual Concepts GmbH, Berlin) for 3D reconstruction.

References

Ahlborn, B. and Werner, D. (1992) 1,3-β-glucan synthase on the peribacteroid membrane (symbiosome membrane) from soybean root nodules. *Physiol. Mol. Plant Pathol.* **40**, 299–314.

Alche, J.D. and Rodriguez-Garcia, M.I. (1997) Fluorochromes for detection of callose in meiocytes of olive (*Olea europea* L.). *Biotechnic. Histochem.* **72**, 285–290.

Alexander, M.P. (1987) A method for staining pollen tubes in pistil. *Stain Technol.* **62**, 107–112.

Benfey, P.N., Linstead, P.J., Roberts, K., Schiefelbein, J.W., Hauser, M.-T. and Aeschbacher, R.A. (1993) Root development in *Arabidopsis*: four mutants with dramatically altered root morphogenesis. *Development*, **119**, 57–70.

Currier, H.B. (1957) Callose substance in plant cells. *Am. J. Bot.* **44**, 478–488.

Dolan, L., Janmaat, K., Willemsen, V., Linstead, P., Poethig, S., Roberts, K. and Scheres, B. (1993) Cellular organisation of the *Arabidopsis thaliana* root. *Development*, **119**, 71–84.

Di Laurenzio, L., Wysocka-Dillar, J., Malamy, J.E., Pysh, L., Helariutta, Y., Freshour, G., Hahn, M.G., Feldmann, K.A. and Benfey, P.N. (1996) The *SCARECROW* gene regulates an asymmetric cell division that is essential for generating the radial organization of the Arabidopsis root. *Cell*, **86**, 423–433.

Haseloff, J. (1999) GFP variants for multispectral imaging of living cells. *Meth. Cell Biol.* **58**, 139–151.

Haseloff, J., Siemering, K.R., Prasher, D.C. and Hodge, S. (1997) Removal of a cryptic intron and subcellular localization of green fluorescent protein are required to mark transgenic *Arabidopsis* plants brightly. *Proc. Natl Acad. Sci. USA*, **94**, 2122–2127.

Helariutta, Y., Fukaki, H., Wysocka-Diller, J., Nakajima, K., Jung, J., Sena, G., Hauser, M.-T. and Benfey, P.N. (2000) The *SHORT-ROOT* gene controls radial patterning of the *Arabidopsis* root through radial signaling. *Cell*, **101**, 555–567.

Kho, Y.O. and Baer, J. (1968) Observing pollen tubes by means of fluorescence. *Euphytica*, **17**, 298–302.

Martin, F.M. (1959) Staining and observing pollen tubes in the style by means of fluorescence. *Stain Technol.* **34**, 436.

Mayer, U., Büttner, G. and Jürgens, G. (1993) Apical-basal pattern formation in the *Arabidopsis* embryo: studies on the role of the *gnom* gene. *Development*, **117**, 149–162.

Nickle, T. and Meinke, D.W. (1998) A cytokinesis-defective mutant of *Arabidopsis* (*cyt1*) characterized by embryonic lethality, incomplete cell walls, and excessive callose accumulation. *Plant J.* **15**, 321–332.

Scheres, B., Di Laurenzio, L., Willemsen, V., Hauser, M.-T., Janmaat, K., Weisbeek, P. and Benfey, P.N. (1995) Mutations affecting the radial organisation of the *Arabidopsis* root display specific defects throughout the embryonic axis. *Development*, **121**, 53–62.

Smith, M.M. and McCully, M.E. (1978) A critical evaluation of the specificity of aniline blue induced fluorescence. *Protoplasma*, **95**, 229–254.

Stone, B.A., Evans, N.A., Bonig, I. and Clarke, A.E. (1984) The application of Sirofluor, a chemically defined fluorochrome from aniline blue for the histochemical detection of callose. *Protoplasma*, **122**, 191–195.

Valvekens, D., van Montagu, M. and van Lijsebettens, M. (1988) *Agrobacterium tumefaciens*-mediated transformation of *Arabidopsis thaliana* root explants by using kanamycin selection. *Proc. Natl Acad. Sci. USA,* **85**, 5536–5540.

van den Berg, C., Willemsen, V., Hage, W., Weisbeek, P. and Scheres, B. (1995) Cell fate in the *Arabidopsis* root determined by directional signalling. *Nature*, **378**, 62–65.

Wysocka-Diller, J.W., Helariutta, Y., Fukaki, H., Malamy, J.E. and Benfey, P.N. (2000) Molecular analysis of SCARECROW function reveals a radial patterning mechanism common to root and shoot. *Development*, **127**, 595–603.